NIH Public Access
Author Manuscript
Neuropsychology. Author manuscript; available in PMC 2012 September 1.

Published in final edited form as:
Neuropsychology. 2011 September ; 25(5): 622–633. doi:10.1037/a0022984.

Psychometrically matched tasks evaluating differential fMRI activation during form and motion processing

Andrea N. Snyder, **Angela M. Hoffa**, and **Thomas M. Talavage**
Purdue University

Mario Dzemidzic, **Donald Wong**, **Mark J. Lowe**, and **Anantha Shekhar**
Indiana University School of Medicine

Brian F. O'Donnell and **Marcie A. Bockbrader**
Indiana University

Abstract

Objective—Deficits in visual perception and working memory are commonly observed in neuropsychiatric disorders and have been investigated using functional MRI. However, interpretation of differences in brain activation may be confounded with differences in task performance between groups. Differences in task difficulty across conditions may also pose interpretative issues in studies of visual processing in healthy subjects.

Method—In order to address these concerns, the present study characterized brain activation in tasks which were psychometrically matched for difficulty. Functional magnetic resonance imaging (fMRI) was used to assess brain activation in ten healthy subjects during discrimination and working memory judgments for static and moving stimuli. For all task conditions, performance accuracy was matched at 70.7%.

Results—Areas associated with V2 and V5 in the dorsal stream were activated during motion processing tasks and V4 in the ventral stream were activated during form processing tasks. Frontoparietal areas associated with working memory were also statistically significant during the working memory tasks.

Conclusions—Application of psychophysical methods to equate task demands provides a practical method to equate performance levels across conditions in fMRI studies, and to compare healthy and cognitively impaired groups at comparable levels of effort. These psychometrically matched tasks can be applied to patients with a variety of cognitive disorders to investigate dysfunction of multiple *a priori* defined brain regions. Measuring the changes in typical activation

Correspondence concerning this article should be addressed to Andrea Snyder, Weldon School of Biomedical Engineering, Purdue University, 206 S. Martin Jischke Drive, West Lafayette, IN 47907. ansnyder@purdue.edu.
Andrea N. Snyder, Weldon School of Biomedical Engineering, Purdue University; Angela M. Hoffa, School of Electrical and Computer Engineering, Purdue University; Thomas M. Talavage, Weldon School of Biomedical Engineering, School of Electrical and Computer Engineering, Purdue University; Mario A. Dzemidzic, Department of Neurology, Indiana University School of Medicine; Donald Wong, Department of Anatomy, Indiana University School of Medicine; Mark J. Lowe, Department of Radiology, Indiana University School of Medicine; Anantha Shekhar, Department of Psychiatry, Indiana University School of Medicine; Brian F. O'Donnell, Department of Psychological and Brain Sciences, Indiana University; Marcie A. Bockbrader, Department of Psychological and Brain Sciences, Indiana University.
Mark J. Lowe is now at Department of Radiology, Cleveland Clinic Foundation. Marcie A. Bockbrader is now at Department of Physical Medicine and Rehabilitation, The Ohio State University.

Publisher's Disclaimer: The following manuscript is the final accepted manuscript. It has not been subjected to the final copyediting, fact-checking, and proofreading required for formal publication. It is not the definitive, publisher-authenticated version. The American Psychological Association and its Council of Editors disclaim any responsibility or liabilities for errors or omissions of this manuscript version, any version derived from this manuscript by NIH, or other third parties. The published version is available at www.apa.org/pubs/journals/neu

NIH-PA Author Manuscript
NIH-PA Author Manuscript
NIH-PA Author Manuscript

NIH-PA Author Manuscript

NIH-PA Author Manuscript

NIH-PA Author Manuscript

patterns in patients with these diseases can be useful for monitoring disease progression, evaluating new drug treatments, and possibly for developing methods for early diagnosis.

Keywords

visual processing; fMRI; working memory; form; motion

Functional magnetic resonance imaging has seen extensive use in comparing cognitive processing between healthy subjects and persons with neuropsychiatric disorders, such as schizophrenia (McGuire, Howes, Stone, & Fusar-Poli, 2008; Sava & Yurgelun-Todd, 2008), Alzheimer's disease (Drzezga, 2008; Sperling, 2007; Wierenga & Bondi, 2007), and Parkinson's disease (Dagher & Nagano-Saito, 2007; van Eimeren & Siebner, 2006). A major aim of this approach is to characterize differences in the amount, location, or connectivity of brain activity between the control and patient groups. However, the interpretation of such differences is often confounded by performance differences between groups, since patients with brain dysfunction often perform more poorly than healthy subjects on cognitive tasks. Individual differences in performance may reflect differences in perceptual processing, attention, learning efficiency, effort, or cognitive strategies. More generally, comparison of fMRI activation between conditions may also be influenced by individual differences in performance. In the visual modality, for example, parametric manipulation of stimulus detectability, decision certainty or effort can have marked effects on activation. Huang et al. (Huang, Xiang, & Cao, 2006) varied the visibility of a target stimulus in a masking paradigm, and found that activation in V1 decreased with decreased stimulus visibility. Volz et al. (Volz, Schubotz, & von Cramon, 2005) showed that increasing uncertainty in a decision making task increased activation within the posterior frontal median cortex. Haynes et al. (Haynes, Driver, & Rees, 2005) reported that the psychometric visibility for target stimuli in a metacontrast paradigm affected effective connectivity between primary visual cortex and the fusiform gyrus. Differences in effort or emotional state may result in variations in the fMRI signal and its intensity during various tasks, including working memory tasks (Banich et al., 2009; Jansma, Ramsey, de Zwart, van Gelderen, & Duyn, 2007; Onoda, Okamoto, & Yamawaki, 2009; Specht, Willmes, Shah, & Jancke, 2003). In conjunction, these findings motivate development of approaches which allow individual calibration of accuracy levels to minimize effects of task performance or stimulus detectability on brain activation. Such matching is critical in the determination of differential deficits – that is, areas or tasks in which patients with the disorder are more affected compared to healthy subjects than in other areas/tasks. Neuroimaging techniques, such as functional magnetic resonance imaging (fMRI), provide a great opportunity to investigate neural processing and strategies used during task execution. Without psychometric matching, however, different performance levels are likely to be associated with different cognitive strategies or activation, potentially negating the value of post hoc correlations of performance with the extent/severity of the disease/disorder.

The Concept of Psychometrically Matched Tasks

One approach to this issue is the use of psychometrically matched tasks, developed such that the difficulty level may be adjusted to achieve a common level of performance across a wide range of abilities. By minimizing the differences between groups resulting from variations in difficulty, one removes a major factor which influences the discriminating power of a task (Chapman & Chapman, 1973). Psychophysical methods which vary the level of noise or contrast in a stimulus allow manipulation of task difficulty or accuracy, ensuring that variations in brain activation between tasks are not a function of difficulty levels. Such psychometrically matched tasks are highly likely to be of benefit in the application of neuroimaging to diseased/disordered states by increasing the likelihood that all subjects are

NIH-PA Author Manuscript

NIH-PA Author Manuscript

NIH-PA Author Manuscript

performing a task using a comparable strategy and are experiencing a comparable emotional/stress load.

Investigation of several disorders such as schizophrenia, Alzheimer's disease, and Parkinson's disease may benefit from the use of psychometrically matched tasks. In all of these disorders, patients exhibit deficits in both visual processing and working memory that may be further studied by comparison between healthy and patient populations using psychometrically matched tasks. Such studies can provide information regarding the physiologic responses associated with both healthy and diseased states.

Goals of the Present Study

This effort seeks to evaluate the use of psychometrically matched tasks by demonstrating that cortical network mapping can be meaningfully affected even when stimuli are allowed to vary on an individual subject basis. By demonstrating areas of activation in healthy controls similar to those expected from previous work on both visual and working memory networks, we can validate these psychometrically matched tasks and their use in neuroimaging. In addition, matching tasks for performance reduces the likelihood that between condition differences are due to non-specific factors such as motivation or task difficulty. Such a protocol as the one described here could be used to further study the diseases described above, as well as many others. Although psychometrically matched tasks have been applied to cognitive assessment in some brain disorders, there are relatively few studies using such tasks in conjunction with fMRI. For example, these matched tasks have demonstrated visual processing deficits in schizophrenic patients compared to healthy subjects; however, these tasks have not yet been used in functional imaging studies (Brenner, Wilt, Lysaker, Koyfman, & O'Donnell, 2003). It is with such applications in mind that we developed this testing protocol and conducted these studies on healthy control volunteers.

Method

Participants

Ten right-handed volunteers participated (six men, four women; age 24–53 years, mean = 42.5 years, standard deviation = 8.9 years). Male and female participants did not significantly differ in terms of age ($t(8) = -0.557$, $p = 0.59$). Participants were screened to exclude a history of neurological disease, psychiatric illness, substance abuse, or corrected eyesight worse than 20/40 as measured with a Snellen eye chart. Potential risks were explained, and informed consent was obtained from participants in accordance with institutional guidelines established by the Indiana University Purdue University at Indianapolis Institutional Review Board.

Stimuli

All conducted experiments presented two or more visual stimuli. First, one of two classes (form or motion) of visual stimuli was presented in varying levels of display noise (see *Display Noise* below). These target stimuli were then followed by a question mark (“?”) prompt during the presentation of which, and prior to commencement of the subsequent trial, subjects were asked to respond by pressing one button on a 4-button response box (Neurostim, Inc.). Form perception tasks used letters D, U, C and L as in Figures 2.2 and 2.4 to maximize the response in the occipitotemporal visual stream regions. Motion perception tasks used random dot patterns with 100 dots as in Figures 2.3 and 2.5 where the dots were either fixed or some portion were moving coherently as described below. This stimulus was specifically designed to stimulate motion specific neural systems in the visual cortex while minimizing position cues (Newsome & Pare, 1988) and is expected to maximize activation

NIH-PA Author Manuscript

NIH-PA Author Manuscript

NIH-PA Author Manuscript

in the occipitoparietal visual stream. All stimuli were shown at high levels of contrast (Michelson contrast > 90%) and presented in a 200×200 pixel rectangular window which subtended 7.5 degrees of visual angle and centered in the subject's field-of-view.

Display Noise

Subject performance was maintained at a constant level through adaptive incorporation of display noise. Therefore, all tasks are matched on visual sensory difficulty. In form perception tasks, visual noise was varied by increasing or decreasing the number of pixels which were randomly assigned the value of black or white. In motion perception tasks, visual noise was varied by increasing or decreasing the number of dots that moved coherently with the pattern. Display noise levels were adjusted throughout practice prior to functional neuroimaging and during imaging runs to maintain performance at the 70.7% level using an up-down staircase method (Levitt, 1971). The behavioral threshold determined prior to functional imaging was used as the initial display noise level in the imaging experiments. During the imaging session, noise levels were adjusted based only on responses made during experimental trials. Responses made during control trials had no effect on levels of display noise. If no response was made to an experimental trial, no display noise adjustment was made. Noise was initially introduced in increments of 5% until the first error was made, following which subsequent changes in noise were in increments of 2%. For both kinds of stimuli, thresholds were calculated from the noise levels of the final four reversals of the staircase. Therefore, thresholds quantified the percent of visual noise in the image at criterion behavioral performance levels.

Tasks

Tests of form and motion perception in noise were adapted for use in the MR scanner based on psychophysical paradigms described by Brenner (Brenner, et al., 2003) and Farmer (Farmer et al., 2000). These behavioral tests were designed to systematically evaluate early stage vision and visual working memory operation. All behavioral tests were implemented for fMRI on a Macintosh computer with screen output through an MR-compatible Avotec viewing system, and subject input was obtained via the button box placed in the right hand. Blocks of experimental and control trials were alternately presented to subjects who were prompted to actively respond to each trial.

During the Form Discrimination condition in Figure 2a, each trial consisted of two visual stimuli: a target stimulus for 400 milliseconds and a prompt for response for 2100 milliseconds. After the prompt, no visual stimulus was presented for 700 milliseconds, resulting in 3200 milliseconds total trial duration. Target stimuli for experimental trials were a letter (“D” or “U”) presented in display noise or display noise only for control trials. In experimental trials, subjects were asked to press button 1, the left-most button, with their index finger if they saw a “D” or button 2, to the right of button 1, with their middle finger if they saw a “U.” In control trials, subjects were instructed to press button 1 after appearance of the prompt.

During the Motion Discrimination condition in Figure 2b, each trial consisted of two visual stimuli: a target stimulus for 400 milliseconds and a prompt for response for 2100 milliseconds. After the prompt, no visual stimulus was presented for 700 milliseconds, resulting in 3200 milliseconds total trial duration. Target stimuli for experimental trials were random dot patterns of which some portion moved in a coherent fashion to the left or right, or random, static dot patterns for the control trials. The velocity of the dots was 7.56 degrees per second. In experimental trials, subjects were instructed to press button 1 if the global direction of motion was to the left or button 2 if it was to the right. In control trials, subjects were instructed to press button 1 after appearance of the prompt.

NIH-PA Author Manuscript

NIH-PA Author Manuscript

NIH-PA Author Manuscript

To achieve activation of working memory networks, delayed-match visual tasks with both form and motion stimuli were created. Working memory in this study is defined as in Cowan et al: "Working memory is the set of mental processes holding limited information in a temporarily accessible state in service of cognition" (Cowan et al., 2005). These working memory tasks are psychometrically matched on sensory difficulty – that is, to increase difficulty of the task, more visual noise is added.

For the Form Working Memory condition in Figure 3a, each trial consisted of three visual stimuli: a target stimulus for 400 milliseconds, a blank screen for 400 milliseconds, a second target stimulus for 400 milliseconds, and a prompt for response for 1500 milliseconds. After the prompt, no visual stimulus was presented for 1300 milliseconds, resulting in 4000 milliseconds total trial duration. The target stimuli for experimental trials were one of four letters (D, U, C, L) presented in display noise. For control trials, the stimulus was display noise only. In experimental trials, subjects were instructed to press button 1 if the two target stimuli were different or button 2 if the target stimuli were the same. In control trials, subjects were instructed to press button 1 after appearance of the prompt.

For the Motion Working Memory condition in Figure 3b, each trial consisted of three visual stimuli: a target stimulus for 400 milliseconds, a blank screen for 400 milliseconds, a second target stimulus for 400 milliseconds, and a prompt for response for 1500 milliseconds. After the prompt, no visual stimulus was presented for 1300 milliseconds, resulting in 4000 milliseconds total trial duration. The target stimuli for experimental trials were random dot patterns, of which some portion exhibited coherent motion to the left, right, up or down, and for control trials were random, static dot patterns. In experimental trials, subjects were instructed to press button 1 if the two target stimuli exhibited different directions of motion or button 2 if the directions of motion were the same. In control trials, subjects were instructed to press button 1 after appearance of the prompt.

Experimental Protocol

The scanning session consisted of a high-resolution anatomical scan followed by four functional imaging runs, one for each experimental condition (Form Discrimination, Form Working Memory, Motion Discrimination, and Motion Working Memory). Each functional imaging run consisted of nine blocks of trials lasting for a total of five minutes and twenty seconds as displayed in Figure 4. Within each run, blocks of tasks alternated between control and experimental trials. The type of block was indicated at the beginning and end of each control block with a duration of 3.2 or 4.0 seconds for discrimination or working memory tasks, respectively, by an instructional cue to the subject: "Press 1" to indicate a control block, and "Press 1 or 2" to indicate an experimental block. The first and last control blocks were 48 seconds long; all other blocks were 32 seconds in duration. Individual discrimination trials had 3.2 seconds duration, so there were 15 discrimination trials in the 48 second control blocks and 10 trials in the 32 second blocks including the instructional cues as trials. Working memory trials were 4 seconds long, so there were 12 trials in the 48 second control blocks and 8 trials in each 32 second block including the instructional cues as trials.

Image Acquisition

Whole-brain imaging was performed using a 1.5T GE Signa LX Horizon MR imager located at the Indiana University School of Medicine (Indianapolis, IN). All images were acquired using a birdcage transmit-receive head coil. For functional imaging runs, 15 contiguous 9 mm thick axial slices were prescribed to image the entire cerebrum and superior aspects of the cerebellum. Each functional run consisted of 160 volumes, acquired using a blood-oxygenation-level-dependent (BOLD) weighted gradient echo echo-planar

NIH-PA Author Manuscript

NIH-PA Author Manuscript

NIH-PA Author Manuscript

imaging sequence with the following imaging parameters: repetition time (TR) = 2 sec; echo time (TE) = 50 ms; acquisition matrix = 64 × 64; flip angle = 90°; field-of-view (FOV) = 240 mm × 240 mm; voxel dimension in the imaging plane 3.75 mm × 3.75 mm. Prior to collecting functional data, high-resolution, anatomic images were acquired in 124 contiguous axial slices using a 3D SPGR sequence (1.1–1.3 millimeter slice thickness; voxel dimension in the imaging plane 256 × 256). These images were collected for purposes of normalization to a standard stereotactic system (Montreal Neurological Institute coordinates). The effects of head motion were minimized by using a head-neck pad and dental bite bar. The average time for the experiment was approximately 1 hour and 45 minutes, including adjusting the visual system goggles, reviewing task directions, all scanning (including additional scans which are not included in this report), and removing the subject from the scanner.

Image Analysis

Image analysis was conducted using the *SPM5* software package (Wellcome Department of Imaging Neuroscience, London, UK). For each subject, functional runs were corrected for slice acquisition timing differences. All image volumes in a functional imaging run were realigned to the second volume of the first functional imaging run (the first volume of each imaging run was discarded to mitigate the effects of the approach to steady-state magnetization signal levels). Nine of the ten subjects showed less than ± 1 mm of head movement in the z direction. The remaining subject exhibited a z-direction drift of almost 3 mm from the original location. Since voxel thickness was large (9 mm) and acquisition slices were contiguous, all data were included. The anatomical SPGR image for each subject was co-registered to the mean functional image of the functional runs and then segmented into its tissue components. Spatial transformation parameters obtained during the segmentation were applied to transform images into the Montreal Neurological Institute (MNI) coordinate space with isotropic voxel dimension of 2 mm. Normalized images were then spatially smoothed using an 8 mm full-width half-maximum (FWHM) Gaussian filter, chosen to reflect functional image resolution and to minimize effects of the inter-subject anatomic variability.

Within-subject analyses were performed for each subject to estimate brain responses to the stimuli by using SPM's informed basis set, which includes the canonical hemodynamic response function and its temporal and dispersion derivatives. The temporal derivatives account for differences in peak response latency while the dispersion derivatives model variations in peak response duration. The first four volumes for each functional run were excluded from this analysis to prevent biases introduced by non-steady state tissue signal levels. The six movement parameters obtained during realignment were included as regressors to account for residual movement-induced effects. A high-pass filter with a cut-off of 1/128 Hz was applied to each voxel's time series to remove low frequency noise. Four basic contrasts were created for each subject (Form, Motion, Discrimination, and Working Memory) using cognitive subtraction. For example, the Form contrast was created by summing the differences between the two form experimental conditions (Form Discrimination and Form Working Memory) and their corresponding control conditions (Figure 5a). The Motion contrast was created similarly using the experimental conditions Motion Discrimination and Motion Working Memory, the Discrimination contrast used the Form Discrimination and Motion Discrimination conditions, and the Working Memory contrast used the Form Working Memory and Motion Working Memory conditions. Random effects analysis was performed using SPM's full factorial model and the informed basis contrast images that were calculated in each subject for each experimental contrast (Motion, Form, Discrimination, and Working Memory) versus their corresponding control condition as described in Figure 5a. Additionally, second level comparisons between

NIH-PA Author Manuscript

NIH-PA Author Manuscript

NIH-PA Author Manuscript

experimental contrasts (Motion > Form, Form > Motion, Discrimination > Working Memory, and Working Memory > Discrimination) were evaluated as illustrated in Figure 5b. For example, the Motion > Form contrast was created by subtracting the Form contrast described above from the Motion contrast.

For each experimental contrast, significantly activated voxels were defined as those within the whole-brain smoothed gray matter mask which satisfied a voxel-wise false discovery rate (FDR) correction, $p_{FDR\text{-}voxel} < 0.05$, and were in clusters exceeding an extent threshold, $k > 40$. For comparisons between experimental contrasts, activated regions were considered at trend-level height ($p < 0.01$, uncorrected) and extent ($k > 20$) thresholds.

Results

Psychometrically Matched Task Performance

All participants were able to maintain a 70.7% accuracy level. Average display noise required to obtain a 70.7% accuracy level on both Discrimination and Working Memory tasks for Form and Motion conditions are shown in Figure 1.

Form, Memory, Working Memory, and Discrimination Contrasts

Areas demonstrating significant activation for the combined experimental contrasts versus their corresponding control contrasts are shown in Tables 1 and 2 and Figure 6. Significantly active areas for the Form contrast included areas of the frontotemporal network and occipitotemporal regions (Table 1). Significant areas in the Motion contrast included bilateral insula, left middle temporal area (MT), left supplemental eye field (SEF), bilateral IFG, bilateral IPL, left middle frontal gyrus (MFG), and left-only FEF. Areas activated in the Working Memory contrast were bilateral insula/frontal operculum, left middle/inferior occipital gyrus (MOG/IOG), bilateral IFG, left SEF, bilateral IPL, right SFG, right thalamus and bilateral FEF. In addition, left declive activation in the cerebellum was also observed. For all contrasts, a left dominance was observed in the IPL, FEF, and visual stream regions.

The data from the Discrimination contrast did not show any significant foci ($p < 0.05$, FDR-corrected for multiple comparisons). However, at a less strict voxel-wise threshold of $p < 0.005$ (uncorrected), activation pattern similar to the working memory task became apparent. Areas included left IPL, bilateral FEF, bilateral insula, left MT, left MOG/IOG, right IFG, left SEF, and right culmen in the cerebellum.

Comparisons between Form and Motion Contrasts

To compare activations between experimental contrasts, the Motion contrast was subtracted from the Form contrast as in Figure 5b and vice versa (Table 2 and Figure 7). The right IOG exhibited greater activation during the Form tasks, while the Motion tasks activated MT bilaterally, left lingual gyri, and left declive.

Comparisons between Working Memory and Discrimination Contrasts

Significant areas of activation during the Working Memory > Discrimination comparison (Table 3, Figure 8) include bilateral IPL and left MFG. No significant activations were seen in the Discrimination > Working Memory comparison.

Discussion

Cognitive subtraction paradigms were used to separate the visual streams and working memory networks. While this method has been shown to be a limitation in distinguishing task-related activation in one network from activation in another network (Friston et al.,

NIH-PA Author Manuscript

NIH-PA Author Manuscript

NIH-PA Author Manuscript

1996), the use of psychometrically matched tasks was not employed. Since the areas that resulted from dorsal, ventral, and working memory networks were those commonly associated with the target network, separating these networks was not limited by cognitive subtraction paradigms using the psychometrically matched tasks.

We will discuss the activation patterns in the Form, Motion, and Working Memory contrasts. This will be followed by a short discussion of potential applications of the protocol to several disease processes as well as clinical considerations.

Form and Motion

Form and Motion contrasts showed areas associated with working memory and with their respective visual stream. As is the case for the Working Memory contrast, both Form and Motion contrasts (when compared with controls) will include working memory components (Figure 5); these areas include the insula, IPL, and IFG (Table 1).

The Form contrast showed activation of V4. This area has been shown to be involved in the ventral stream of the visual processing network, activated by object recognition tasks. In addition, activation in the MOG has been shown during reading and letter identification tasks, which is essentially the task used in the current protocol described in this study (Cornelissen et al., 2009; Pernet et al., 2004; Turkeltaub, Flowers, Lyon, & Eden, 2008). The Form contrast also activated the SFG, which has also been shown to be a part of the ventral form processing stream. Activation of the culmen was also seen. As part of the cerebellum, it is possible that activation in this area is due to residual effects from working memory tasks known to activate areas of the cerebellum. Alternatively, culmen activity is found to be correlated with optic processing, including saccades and maintenance of attention (Dieterich, Bucher, Seelos, & Brandt, 2000). Finally, activation of the ITG was seen, which is in agreement with many studies showing this region to be important in higher levels of form processing in the ventral stream (Gerlach et al., 2002; Gulyas, Heywood, Popplewell, Roland, & Cowey, 1994; Gulyas & Roland, 1991; Jastorff & Orban, 2009).

The Motion contrast showed both left MT, an area associated with V5, and left cerebellum, an area associated with visual motion tasks. MT is one of the main areas associated with visual motion processing in the dorsal stream, with areas specific to speed, direction, and other parameters as shown by many techniques, including fMRI (Bartels, Logothetis, & Moutoussis, 2008; Born & Bradley, 2005; Giaschi, Zwicker, Young, & Bjornson, 2007; Martinez-Trujillo et al., 2005). In addition, the cerebellum has been shown to be involved in motion processing (Bronstein, Grunfeld, Faldon, & Okada, 2008; Dupont, Orban, De Bruyn, Verbruggen, & Mortelmans, 1994; Nawrot & Rizzo, 1998). The identification of these areas in form and motion processing demonstrates that this protocol is an effective probe of the ventral and dorsal visual processing networks.

Comparisons then showed the areas specific to each contrast. Form > Motion showed right V4 as expected. Motion > Form successfully showed left lingual gyrus (V2) and bilateral V5 regions, as well as left cerebellum, as expected from the basic areas involved in the ventral and dorsal visual processing streams (Livingstone & Hubel, 1988; Paradis et al., 2000; Tootell, Dale, Sereno, & Malach, 1996). Left dominance in the IPL and FEF regions for the single Motion, Form, and Working Memory contrasts may be due to the subjects being right-handed. While the left dominance appears in the single contrasts, it does not in the comparison contrasts.

Region of Interest Analysis of ITG for Laterality

An ROI analysis was performed on the Inferior Temporal Gyrus (ITG). The percent signal change from this area was calculated bilaterally for the Form contrast to further show left

NIH-PA Author Manuscript

NIH-PA Author Manuscript

NIH-PA Author Manuscript

dominance for the Form contrast in this area. A 10 mm × 10 mm × 10 mm cube was centered on the and ITG. The boundary according to the MarsBaR analysis toolbox (Brett, Anton, Valabregue, & Poline, 2002) between the MT, ITG, and Middle Occipital Gyrus (MOG) was approximately consistent with the functional boundary between the left FG cluster for Form. The cube was centered 5 mm above and below this boundary. Raw signal data was then extracted for bilateral ITG ROIs for a total of two ROIs per subject. The information corresponding to each condition (Form Working Memory, Form Discrimination) was averaged for each ROI for every subject.

A two-way analysis of variance (ANOVA) was performed across condition (Working Memory and Discrimination) as well as laterality (Right and Left). ITG signal change was significantly different for both the Working Memory and Discrimination comparison and the laterality comparison. This information further supports the idea of a left bias for the Form Working Memory condition.

Working Memory

Typical working memory networks were shown to be activated by this protocol, validating the tasks as an appropriate probe of visual working memory. When evaluating the Working Memory contrast, we expect to see activation of both the Form and Motion networks, since our paradigm combines the Form Working Memory and Motion Working Memory conditions (for example, see Figure 5). This explains the left MOG and left Cerebellum clusters, areas associated with Form and Motion, respectively (Table 1). As expected, these clusters disappear in the Working Memory > Discrimination comparison, as this subtraction cancels out effects from Form and Motion tasks. It has also been suggested that visual working memory networks, like visual processing networks, may be divided into the two separate processing streams (Jennings, van der Veen, & Meltzer, 2006;Muller & Knight, 2006), possibly explaining the activation of these areas.

Left dominance in the MFG area during the Working Memory > Discrimination comparison may also be explained by the right-handedness of the subjects. Alternatively, it has been seen that working memory tasks can display left dominance in frontal regions, regardless of handedness (Coull, Frith, Frackowiak, & Grasby, 1996).

Other areas activated in the Working Memory contrast agree with previous imaging studies of working memory. Brodmann's area 40 (here referred to as the inferior parietal lobe) shows activation in the Working Memory contrast and is involved in the working memory and attention networks (Cohen et al., 1997; Muller & Knight, 2006). The MFG, activated in this study in the Working Memory > Discrimination contrast (Table 3), has been shown to be involved in working memory processing (D'Esposito et al., 1998; McCarthy et al., 1996). The cerebellum, which also showed activation in the Working Memory contrast, specifically in the declive (Table 1), has also been shown to be involved in working memory (Hautzel, Mottaghy, Specht, Muller, & Krause, 2009). In addition, the thalamus is involved in working memory and has many neural connections with other areas in the working memory network (Constantinidis & Procyk, 2004; Hartley & Speer, 2000). The thalamus showed activation in the Working Memory contrast, and this activation cluster was not seen in any other contrast. Finally, the Working Memory contrast showed areas associated with working memory, attention, and decision-making including the insula, FEF, and IFG (Curtis, 2006; LaBar, Gitelman, Parrish, & Mesulam, 1999).

The Working Memory > Discrimination contrast allowed for separation of working memory networks from the visual processing networks used in the Form and Motion tasks. This contrast showed activation clusters in the left MFG and bilateral IPL, two areas strongly related to working memory processing.

NIH-PA Author Manuscript

NIH-PA Author Manuscript

NIH-PA Author Manuscript

Psychometrically Matched Tasks

The use of psychometrically matched tasks to control the task difficulty for individuals demonstrated variation between subjects. However, it was shown that the tasks can be matched on difficulty in real-time as the subjects are performing the experiment in an fMRI machine. Psychometrically matched tasks are used commonly in cognitive testing in disease (for example, in schizophrenia (Brenner, et al., 2003) and dementia (Mungas, Reed, & Kramer, 2003; Trick & Silverman, 1991)); however, the use of psychometrically matched tasks in fMRI studies is rare. A previous study used fMRI and psychometrically matched stimuli to study language processing (Spitzer et al., 1996); however, to the authors' knowledge, no study using fMRI to study visual form and motion processing and working memory networks has yet been conducted with psychometrically matched tasks.

Potential Application to Visual Processing Deficits

Schizophrenia, Alzheimer's disease and Parkinson's disease are all associated with visual processing deficits of form, motion, or both. Schizophrenia patients show disturbances of early stage vision indicative of the retinogeniculate pathway, occipital cortex, or cerebellar disruption (Chen et al., 1999; Slaghuis, 1998). and are more profound for stimuli and tasks involving motion compared to form perception (Brenner, Lysaker, Wilt, & O'Donnell, 2002; O'Donnell et al., 1996). Alzheimer's patients displayed increased difficulty with radial motion detection when compared with age-matched older adult controls (Fernandez, Kavcic, & Duffy, 2007; Mapstone, Dickerson, & Duffy, 2008), while horizontal motion discrimination showed no difference between Alzheimer disease patients and age-matched adult controls (Mapstone, et al., 2008). Parkinson's disease has also been shown to be associated with visual deficits (Arakawa, Tobimatsu, Kato, & Kira, 1999; Castelo-Branco et al., 2009; Trick, Kaskie, & Steinman, 1994), largely related, according to evoked-related potential studies, to the magnocellular (time-varying visual stimulus processing) pathway rather than the parvocellular (form and color processing) pathway (Arakawa, et al., 1999). By demonstrating activation of these visual processing form and motion networks in healthy subjects with a psychometrically matched task, we both validate the protocol as an appropriate probe of visual processing and determine typical activation patterns with which to compare a clinical population.

Potential Application to Working Memory Deficits

Working memory deficits are also reported for schizophrenia dysfunction (Cuesta, Peralta, & Juan, 1996; Reichenberg, 2010; Silver, Feldman, Bilker, & Gur, 2003; Tek et al., 2002), Alzheimer's disease (Germano, Kinsella, Storey, Ong, & Ames, 2008; Huntley & Howard), and Parkinson's disease (Bradley, Welch, & Dick, 1989; Dubois & Pillon, 1997; Lee et al., 2010). For example, it is proposed that Alzheimer patients' inability to learn new information is likely to be due to deficits in working memory (Germano & Kinsella, 2005). As with the visual processing tasks, studying the effects of a working memory load on the psychometrically matched tasks in healthy subjects is also essential. The use of psychometrically matched tasks to study working memory networks may allow more accurate comparison of disorders. For example, although both Parkinson's and Alzheimer's diseases show difficulties with working memory, these deficits may not be due to dysfunction in the same areas of the brain (Kensinger, Shearer, Locascio, Growdon, & Corkin, 2003). This protocol may be useful in elucidating differences in the source of working memory deficits in these and other disorders which affect working memory networks.

NIH-PA Author Manuscript

NIH-PA Author Manuscript

NIH-PA Author Manuscript

Clinical Translation

There are a few considerations that should be addressed to translate this protocol into clinical use. First, the time necessary to scan each individual should be reduced. This may be accomplished in two ways: by identifying clinically relevant task conditions for certain diseases and by reducing the number of stimulus presentations for each task. Although the number of stimulus presentations here was chosen to increase the chances of obtaining useful data, it is possible that this approach was conservative, particularly with the increased availability of higher-field imaging.

In addition, although participants in this study spanned a wide range of ages, more research is required on the effects of age on brain activation patterns obtained using this protocol. It is known that memory performance and brain activation changes with even healthy aging (Buckner, 2004). Further, the BOLD signal itself may be affected by aging (D'Esposito, Zarahn, Aguirre, & Rypma, 1999; Huettel, Singerman, & McCarthy, 2001). Therefore, for this protocol to be useful in a clinical environment, healthy activation patterns for several age groups will be required for comparison with patients.

This protocol is fairly simple and may be performed by patients with a wide variety of ability levels due to the difficulty-matched tasks. These tasks have been used to study schizophrenia and schizotypal personality disorder, Huntington's disease, and autism (Brenner, et al., 2003; Davis, Bockbrader, Murphy, Hetrick, & O'Donnell, 2006; O'Donnell et al., 2006; O'Donnell et al., 2008).

Conclusions

The use of four psychometrically matched tasks allowed successful separation of the working memory networks and visual stream regions. Differential areas of activation from the Form and Motion comparison contrasts can be isolated as important processing centers and compared in later studies with areas activated in a patient population.

Key areas in the working memory network were also successfully demonstrated. Therefore, the differential working memory comparison to discrimination tasks is still a valid identification of key areas during the working memory process. Overall, these psychometrically matched tasks elicit expected responses in healthy subjects that maybe be used to study the hypothesized areas of dysfunction in many cognitive and psychological disorders.

Acknowledgments

This publication was supported in part by NIMH Grant Number R01 MH62150 (BFO). Its contents are solely the responsibility of the authors and do not necessarily represent the official views of the NIH. Additional support provided by PHS (NCCR) Grant Number 5TL1RR025759-02 (A. Shekhar).

References

Arakawa K, Tobimatsu S, Kato M, Kira J. Parvocellular and magnocellular visual processing in spinocerebellar degeneration and Parkinson's disease: an event-related potential study. Clin Neurophysiol. 1999; 110(6):1048–1057. [PubMed: 10402092]

Banich MT, Mackiewicz KL, Depue BE, Whitmer AJ, Miller GA, Heller W. Cognitive control mechanisms, emotion and memory: A neural perspective with implications for psychopathology. Neuroscience and Biobehavioral Reviews. 2009; 33(5):613–630. [PubMed: 18948135]

Bartels A, Logothetis NK, Moutoussis K. fMRI and its interpretations: an illustration on directional selectivity in area V5/MT. Trends Neurosci. 2008; 31(9):444–453. [PubMed: 18676033]

NIH-PA Author Manuscript

NIH-PA Author Manuscript

NIH-PA Author Manuscript

Born RT, Bradley DC. Structure and function of visual area MT. Annu Rev Neurosci. 2005; 28:157–189. [PubMed: 16022593]

Bradley VA, Welch JL, Dick DJ. Visuospatial working memory in Parkinson's disease. J Neurol Neurosurg Psychiatry. 1989; 52(11):1228–1235. [PubMed: 2592967]

Brenner CA, Lysaker PH, Wilt MA, O'Donnell BF. Visual processing and neuropsychological function in schizophrenia and schizoaffective disorder. Psychiatry Res. 2002; 111(2–3):125–136. [PubMed: 12374630]

Brenner CA, Wilt MA, Lysaker PH, Koyfman A, O'Donnell BF. Psychometrically matched visual-processing tasks in schizophrenia spectrum disorders. J Abnorm Psychol. 2003; 112(1):28–37. [PubMed: 12653411]

Brett, M.; Anton, JL.; Valabregue, R.; Poline, JB. Region of interest analysis using an SPM toolbox. Available on CD-ROM in NeuroImage; 8th International Conference on Functional Mapping of the Human Brain; Sendai, Japan. June 2—6, 2002; 2002. abstract

Bronstein AM, Grunfeld EA, Faldon M, Okada T. Reduced self-motion perception in patients with midline cerebellar lesions. Neuroreport. 2008; 19(6):691–693. [PubMed: 18382289]

Buckner RL. Memory and executive function in aging and AD: multiple factors that cause decline and reserve factors that compensate. Neuron. 2004; 44(1):195–208. [PubMed: 15450170]

Castelo-Branco M, Mendes M, Silva F, Massano J, Januario G, Januario C. Motion integration deficits are independent of magnocellular impairment in Parkinson's disease. Neuropsychologia. 2009; 47(2):314–320. [PubMed: 18822307]

Chapman LJ, Chapman JP. Problems in the measurement of cognitive deficit. Psychol Bull. 1973; 79(6):380–385. [PubMed: 4707457]

Chen Y, Palafox GP, Nakayama K, Levy DL, Matthysse S, Holzman PS. Motion perception in schizophrenia. Arch Gen Psychiatry. 1999; 56(2):149–154. [PubMed: 10025439]

Cohen JD, Perlstein WM, Braver TS, Nystrom LE, Noll DC, Jonides J. Temporal dynamics of brain activation during a working memory task. Nature. 1997; 386(6625):604–608. [PubMed: 9121583]

Constantinidis C, Procyk E. The primate working memory networks. Cogn Affect Behav Neurosci. 2004; 4(4):444–465. [PubMed: 15849890]

Cornelissen P, Kringelbach M, Ellis A, Whitney C, Holliday I, Hansen P. Activation of the left inferior frontal gyrus in the first 200 ms of reading: evidence from magnetoencephalography (MEG). PLoS One. 2009; 4(4)

Coull JT, Frith CD, Frackowiak RS, Grasby PM. A fronto-parietal network for rapid visual information processing: a PET study of sustained attention and working memory. Neuropsychologia. 1996; 34(11):1085–1095. [PubMed: 8904746]

Cowan N, Elliott EM, Scott Saults J, Morey CC, Mattox S, Hismjatullina A. On the capacity of attention: its estimation and its role in working memory and cognitive aptitudes. Cogn Psychol. 2005; 51(1):42–100. [PubMed: 16039935]

Cuesta MJ, Peralta V, Juan JA. Abnormal subjective experiences in schizophrenia: its relationships with neuropsychological disturbances and frontal signs. Eur Arch Psychiatry Clin Neurosci. 1996; 246(2):101–105. [PubMed: 9063905]

Curtis CE. Prefrontal and parietal contributions to spatial working memory. Neuroscience. 2006; 139(1):173–180. [PubMed: 16326021]

D'Esposito M, Aguirre GK, Zarahn E, Ballard D, Shin RK, Lease J. Functional MRI studies of spatial and nonspatial working memory. Brain Res Cogn Brain Res. 1998; 7(1):1–13. [PubMed: 9714705]

D'Esposito M, Zarahn E, Aguirre GK, Rypma B. The effect of normal aging on the coupling of neural activity to the bold hemodynamic response. NeuroImage. 1999; 10(1):6–14. [PubMed: 10385577]

Dagher A, Nagano-Saito A. Functional and anatomical magnetic resonance imaging in Parkinson's disease. Molecular Imaging and Biology. 2007; 9(4):234–242. [PubMed: 17318668]

Davis RA, Bockbrader MA, Murphy RR, Hetrick WP, O'Donnell BF. Subjective perceptual distortions and visual dysfunction in children with autism. J Autism Dev Disord. 2006; 36(2):199–210. [PubMed: 16453070]

Dieterich M, Bucher SF, Seelos KC, Brandt T. Cerebellar activation during optokinetic stimulation and saccades. Neurology. 2000; 54(1):148–155. [PubMed: 10636141]

NIH-PA Author Manuscript

NIH-PA Author Manuscript

NIH-PA Author Manuscript

Drzezga A. Concept of functional imaging of memory decline in Alzheimer's disease. Methods. 2008; 44(4):304–314. [PubMed: 18374274]

Dubois B, Pillon B. Cognitive deficits in Parkinson's disease. J Neurol. 1997; 244(1):2–8. [PubMed: 9007738]

Dupont P, Orban GA, De Bruyn B, Verbruggen A, Mortelmans L. Many areas in the human brain respond to visual motion. J Neurophysiol. 1994; 72(3):1420–1424. [PubMed: 7807222]

Farmer CM, O'Donnell BF, Niznikiewicz MA, Voglmaier MM, McCarley RW, Shenton ME. Visual perception and working memory in schizotypal personality disorder. Am J Psychiatry. 2000; 157(5):781–788. [PubMed: 10784472]

Fernandez R, Kavcic V, Duffy CJ. Neurophysiologic analyses of low- and high-level visual processing in Alzheimer disease. Neurology. 2007; 68(24):2066–2076. [PubMed: 17562827]

Friston KJ, Price CJ, Fletcher P, Moore C, Frackowiak RS, Dolan RJ. The trouble with cognitive subtraction. Neuroimage. 1996; 4(2):97–104. [PubMed: 9345501]

Gerlach C, Aaside CT, Humphreys GW, Gade A, Paulson OB, Law I. Brain activity related to integrative processes in visual object recognition: bottom-up integration and the modulatory influence of stored knowledge. Neuropsychologia. 2002; 40(8):1254–1267. [PubMed: 11931928]

Germano C, Kinsella GJ. Working memory and learning in early Alzheimer's disease. Neuropsychol Rev. 2005; 15(1):1–10. [PubMed: 15929495]

Germano C, Kinsella GJ, Storey E, Ong B, Ames D. The episodic buffer and learning in early Alzheimer's disease. J Clin Exp Neuropsychol. 2008; 30(6):627–638. [PubMed: 18612873]

Giaschi D, Zwicker A, Young SA, Bjornson B. The role of cortical area V5/MT+ in speed-tuned directional anisotropies in global motion perception. Vision Res. 2007; 47(7):887–898. [PubMed: 17306855]

Gulyas B, Heywood CA, Popplewell DA, Roland PE, Cowey A. Visual form discrimination from color or motion cues: functional anatomy by positron emission tomography. Proc Natl Acad Sci U S A. 1994; 91(21):9965–9969. [PubMed: 7937927]

Gulyas B, Roland PE. Cortical fields participating in form and colour discrimination in the human brain. Neuroreport. 1991; 2(10):585–588. [PubMed: 1756239]

Hartley AA, Speer NK. Locating and fractionating working memory using functional neuroimaging: storage, maintenance, and executive functions. Microsc Res Tech. 2000; 51(1):45–53. [PubMed: 11002352]

Hautzel H, Mottaghy FM, Specht K, Muller HW, Krause BJ. Evidence of a modality-dependent role of the cerebellum in working memory? An fMRI study comparing verbal and abstract n-back tasks. Neuroimage. 2009; 47(4):2073–2082. [PubMed: 19524048]

Haynes JD, Driver J, Rees G. Visibility reflects dynamic changes of effective connectivity between V1 and fusiform cortex. Neuron. 2005; 46(5):811–821. [PubMed: 15924866]

Huang J, Xiang M, Cao Y. Reduction in V1 activation associated with decreased visibility of a visual target. Neuroimage. 2006; 31(4):1693–1699. [PubMed: 16603387]

Huettel SA, Singerman JD, McCarthy G. The effects of aging upon the hemodynamic response measured by functional MRI. NeuroImage. 2001; 13(1):161–175. [PubMed: 11133319]

Huntley JD, Howard RJ. Working memory in early Alzheimer's disease: a neuropsychological review. Int J Geriatr Psychiatry. 25(2):121–132. [PubMed: 19672843]

Jansma JM, Ramsey NF, de Zwart JA, van Gelderen P, Duyn JH. fMRI study of effort and information processing in a working memory task. Hum Brain Mapp. 2007; 28(5):431–440. [PubMed: 17133397]

Jastorff J, Orban GA. Human functional magnetic resonance imaging reveals separation and integration of shape and motion cues in biological motion processing. J Neurosci. 2009; 29(22): 7315–7329. [PubMed: 19494153]

Jennings JR, van der Veen FM, Meltzer CC. Verbal and spatial working memory in older individuals: A positron emission tomography study. Brain Res. 2006; 1092(1):177–189. [PubMed: 16709401]

Kensinger EA, Shearer DK, Locascio JJ, Growdon JH, Corkin S. Working memory in mild Alzheimer's disease and early Parkinson's disease. Neuropsychology. 2003; 17(2):230–239. [PubMed: 12803428]

NIH-PA Author Manuscript

NIH-PA Author Manuscript

NIH-PA Author Manuscript

LaBar KS, Gitelman DR, Parrish TB, Mesulam M. Neuroanatomic overlap of working memory and spatial attention networks: a functional MRI comparison within subjects. Neuroimage. 1999; 10(6):695–704. [PubMed: 10600415]

Lee EY, Cowan N, Vogel EK, Rolan T, Valle-Inclan F, Hackley SA. Visual working memory deficits in patients with Parkinson's disease are due to both reduced storage capacity and impaired ability to filter out irrelevant information. Brain. 2010; 133(9):2677–2689. [PubMed: 20688815]

Levitt H. Transformed up-down methods in psychoacoustics. J Acoust Soc Am. 1971; 49(2)(Suppl 2): 467+. [PubMed: 5541744]

Livingstone M, Hubel D. Segregation of form, color, movement, and depth: anatomy, physiology, and perception. Science. 1988; 240(4853):740–749. [PubMed: 3283936]

Mapstone M, Dickerson K, Duffy CJ. Distinct mechanisms of impairment in cognitive ageing and Alzheimer's disease. Brain. 2008; 131(Pt 6):1618–1629. [PubMed: 18385184]

Martinez-Trujillo JC, Tsotsos JK, Simine E, Pomplun M, Wildes R, Treue S. Selectivity for speed gradients in human area MT/V5. Neuroreport. 2005; 16(5):435–438. [PubMed: 15770147]

McCarthy G, Puce A, Constable RT, Krystal JH, Gore JC, Goldman-Rakic P. Activation of human prefrontal cortex during spatial and nonspatial working memory tasks measured by functional MRI. Cereb Cortex. 1996; 6(4):600–611. [PubMed: 8670685]

McGuire P, Howes OD, Stone J, Fusar-Poli P. Functional neuroimaging in schizophrenia: diagnosis and drug discovery. Trends Pharmacol Sci. 2008; 29(2):91–98. [PubMed: 18187211]

Muller NG, Knight RT. The functional neuroanatomy of working memory: contributions of human brain lesion studies. Neuroscience. 2006; 139(1):51–58. [PubMed: 16352402]

Mungas D, Reed BR, Kramer JH. Psychometrically matched measures of global cognition, memory, and executive function for assessment of cognitive decline in older persons. Neuropsychology. 2003; 17(3):380–392. [PubMed: 12959504]

Nawrot M, Rizzo M. Chronic motion perception deficits from midline cerebellar lesions in human. Vision Res. 1998; 38(14):2219–2224. [PubMed: 9797981]

Newsome WT, Pare EB. A selective impairment of motion perception following lesions of the middle temporal visual area (MT). J Neurosci. 1988; 8(6):2201–2211. [PubMed: 3385495]

O'Donnell BF, Bismark A, Hetrick WP, Bodkins M, Vohs JL, Shekhar A. Early stage vision in schizophrenia and schizotypal personality disorder. Schizophr Res. 2006; 86(1–3):89–98. [PubMed: 16829048]

O'Donnell BF, Blekher TM, Weaver M, White KM, Marshall J, Beristain X. Visual perception in prediagnostic and early stage Huntington's disease. J Int Neuropsychol Soc. 2008; 14(3):446–453. [PubMed: 18419843]

O'Donnell BF, Swearer JM, Smith LT, Nestor PG, Shenton ME, McCarley RW. Selective deficits in visual perception and recognition in schizophrenia. Am J Psychiatry. 1996; 153(5):687–692. [PubMed: 8615416]

Onoda K, Okamoto Y, Yamawaki S. Neural correlates of associative memory: The effects of negative emotion. Neuroscience Research. 2009; 64(1):50–55. [PubMed: 19428683]

Paradis AL, Cornilleau-Peres V, Droulez J, Van De Moortele PF, Lobel E, Berthoz A. Visual perception of motion and 3-D structure from motion: an fMRI study. Cereb Cortex. 2000; 10(8): 772–783. [PubMed: 10920049]

Pernet C, Franceries X, Basan S, Cassol E, Démonet J, Celsis P. Anatomy and time course of discrimination and categorization processes in vision: an fMRI study. NeuroImage. 2004; 22(4): 1563–1577. [PubMed: 15275913]

Reichenberg A. The assessment of neuropsychological functioning in schizophrenia. Dialogues Clin Neurosci. 2010; 12(3):383–392. [PubMed: 20954432]

Sava S, Yurgelun-Todd DA. Functional magnetic resonance in psychiatry. Top Magn Reson Imaging. 2008; 19(2):71–79. [PubMed: 19363430]

Silver H, Feldman P, Bilker W, Gur RC. Working memory deficit as a core neuropsychological dysfunction in schizophrenia. Am J Psychiatry. 2003; 160(10):1809–1816. [PubMed: 14514495]

Slaghuis WL. Contrast sensitivity for stationary and drifting spatial frequency gratings in positive- and negative-symptom schizophrenia. J Abnorm Psychol. 1998; 107(1):49–62. [PubMed: 9505038]

NIH-PA Author Manuscript

NIH-PA Author Manuscript

NIH-PA Author Manuscript

Specht K, Willmes K, Shah NJ, Jancke L. Assessment of reliability in functional imaging studies. J Magn Reson Imaging. 2003; 17(4):463–471. [PubMed: 12655586]

Sperling R. Functional MRI studies of associative encoding in normal aging, mild cognitive impairment, and Alzheimer's disease. Ann N Y Acad Sci. 2007; 1097:146–155. [PubMed: 17413017]

Spitzer M, Bellemann ME, Kammer T, Guckel F, Kischka U, Maier S. Functional MR imaging of semantic information processing and learning-related effects using psychometrically controlled stimulation paradigms. Brain Res Cogn Brain Res. 1996; 4(3):149–161. [PubMed: 8924044]

Tek C, Gold J, Blaxton T, Wilk C, McMahon RP, Buchanan RW. Visual perceptual and working memory impairments in schizophrenia. Arch Gen Psychiatry. 2002; 59(2):146–153. [PubMed: 11825136]

Tootell RB, Dale AM, Sereno MI, Malach R. New images from human visual cortex. Trends Neurosci. 1996; 19(11):481–489. [PubMed: 8931274]

Trick GL, Kaskie B, Steinman SB. Visual impairment in Parkinson's disease: deficits in orientation and motion discrimination. Optom Vis Sci. 1994; 71(4):242–245. [PubMed: 8047335]

Trick GL, Silverman SE. Visual sensitivity to motion: age-related changes and deficits in senile dementia of the Alzheimer type. Neurology. 1991; 41(9):1437–1440. [PubMed: 1891094]

Turkeltaub PE, Flowers DL, Lyon LG, Eden GF. Development of ventral stream representations for single letters. Ann N Y Acad Sci. 2008; 1145:13–29. [PubMed: 19076386]

van Eimeren T, Siebner HR. An update on functional neuroimaging of parkinsonism and dystonia. Current Opinion in Neurology. 2006; 19(4):412–419. [PubMed: 16914982]

Volz KG, Schubotz RI, von Cramon DY. Variants of uncertainty in decision-making and their neural correlates. Brain Res Bull. 2005; 67(5):403–412. [PubMed: 16216687]

Wierenga CE, Bondi MW. Use of functional magnetic resonance imaging in the early identification of Alzheimer's disease. Neuropsychology Review. 2007; 17(2):127–143. [PubMed: 17476598]

NIH-PA Author Manuscript
NIH-PA Author Manuscript
NIH-PA Author Manuscript

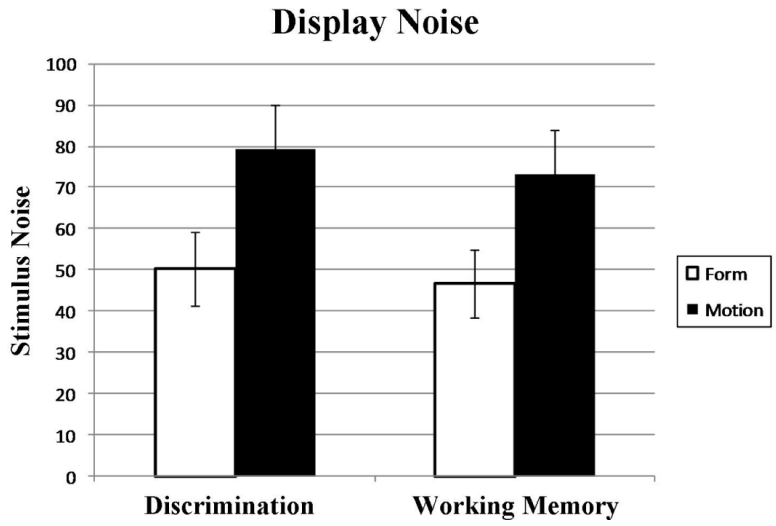

Figure 1.

Average display noise present in stimuli during fMRI experiments. Display noise in the Form condition is the percentage of pixels that were randomly assigned the value of black or white. Display noise in the Motion condition is the percentage of dots that did not move coherently with the pattern.

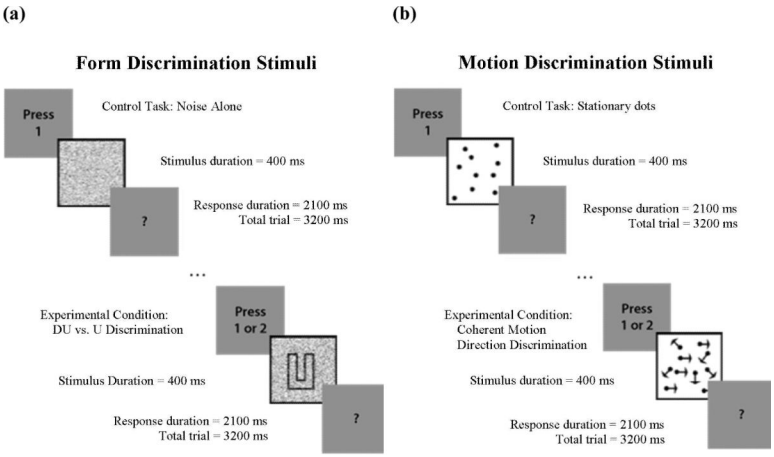

Figure 2.
Cartoons depicting discrimination tasks for (a) Form and (b) Motion

NIH-PA Author Manuscript
NIH-PA Author Manuscript
NIH-PA Author Manuscript

NIH-PA Author Manuscript

NIH-PA Author Manuscript

NIH-PA Author Manuscript

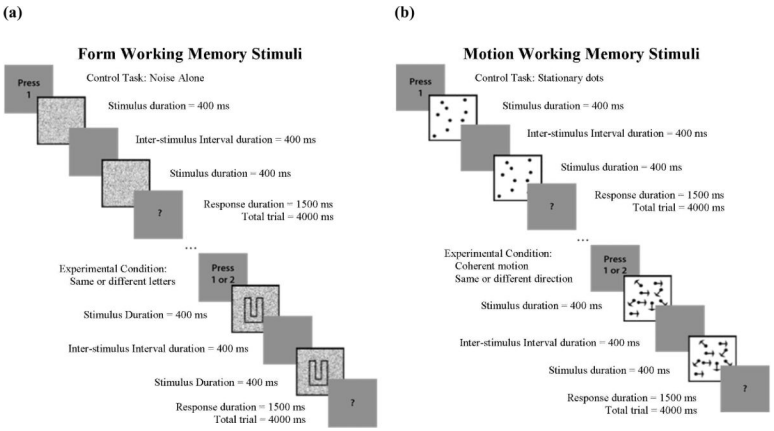

Figure 3.
Cartoons depicting working memory tasks for (a) Form and (b) Motion

NIH-PA Author Manuscript

NIH-PA Author Manuscript

NIH-PA Author Manuscript

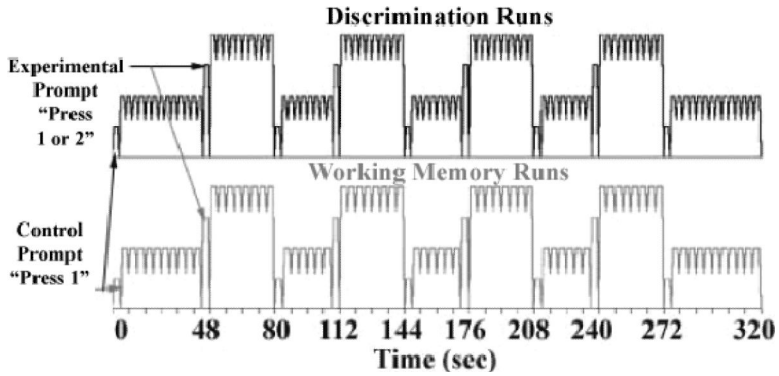

Figure 4.
Experimental blocked paradigm. Instructional prompts were issued at the beginning and end of each control block for the length of a stimulus trial.

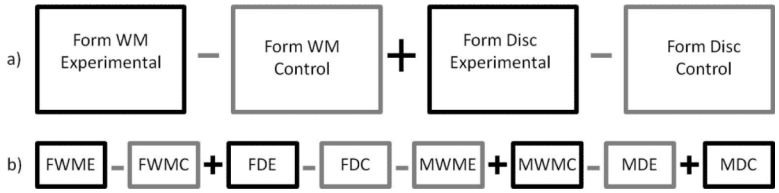

Figure 5.

Contrast examples. a) Form contrast and b) Form > Motion contrast. Abbreviations: WM = Working Memory, D = Discrimination, F = Form, M = Motion, E = Experimental Condition, C = Control Condition.

NIH-PA Author Manuscript
NIH-PA Author Manuscript
NIH-PA Author Manuscript

NIH-PA Author Manuscript
NIH-PA Author Manuscript
NIH-PA Author Manuscript

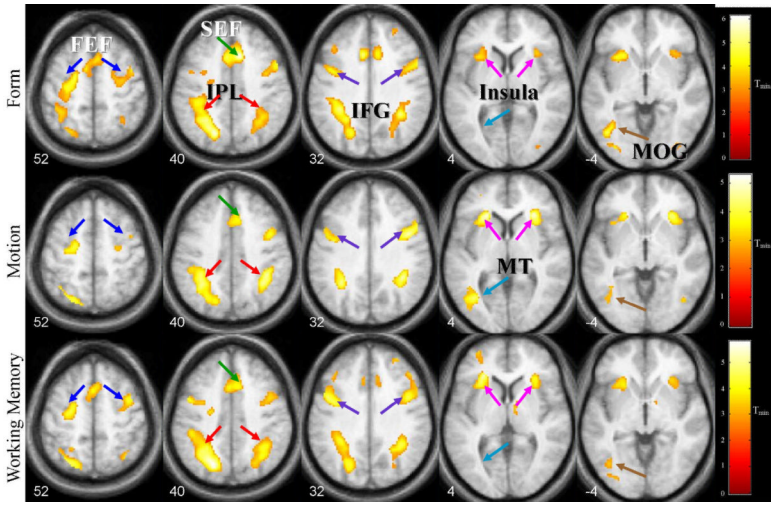

Figure 6.

Areas activated during Form, Motion, and Working Memory contrasts at voxel-wise FDR-corrected $p < 0.05$ and extent threshold $k > 40$. Z-coordinates indicate locations in MNI space. Abbreviations: FEF = frontal eye field, SEF = supplemental eye field, IPL = inferior parietal lobule, IFG = inferior frontal gyrus, MT = middle temporal area, MOG = middle occipital gyrus

NIH-PA Author Manuscript
NIH-PA Author Manuscript
NIH-PA Author Manuscript

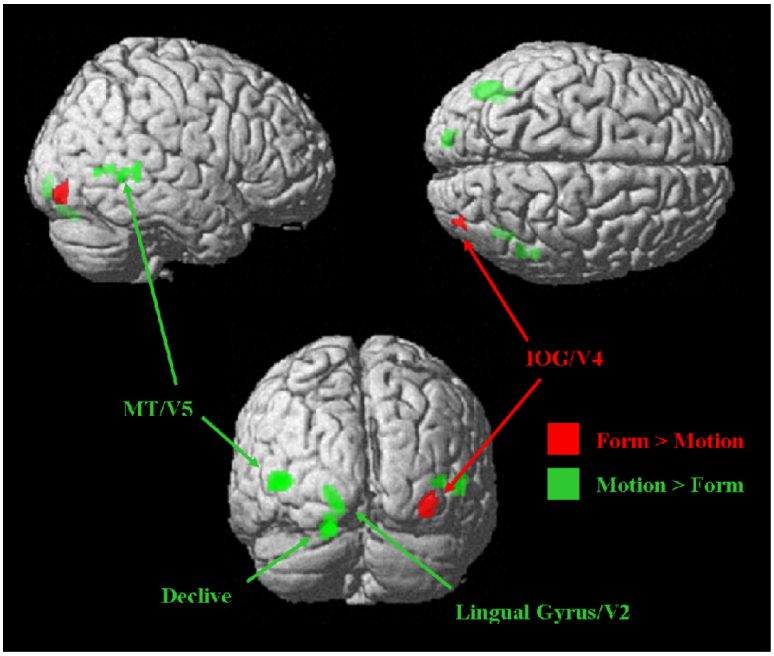

Figure 7.
Areas differentially activated in Form and Motion contrasts at a trend-level display threshold, $p < 0.001$ (uncorrected) and extent threshold, $k > 20$. Abbreviations: MT = middle temporal area, IOG = inferior occipital gyrus.

NIH-PA Author Manuscript
NIH-PA Author Manuscript
NIH-PA Author Manuscript

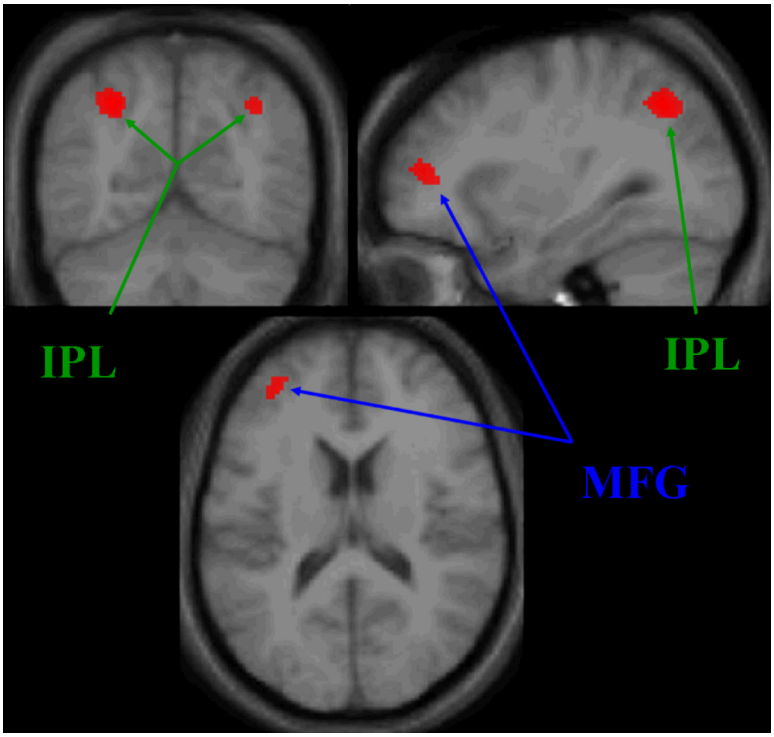

Figure 8.
Working memory network (Working Memory > Discrimination contrast). Trend-level display threshold of $p < 0.001$ (uncorrected) and an extent threshold, $k > 20$ Abbreviations: MFG = middle frontal gyrus, IPL = inferior parietal lobule.

NIH-PA Author Manuscript NIH-PA Author Manuscript NIH-PA Author Manuscript

Table 1

Loci of activation in Form, Motion, and Working Memory contrasts determined at an FDR-corrected display threshold of $p < 0.05$ and extent threshold, $k > 40$. Coordinates in MNI. Size of cluster (number of voxels) and Z scores are also included. Abbreviations: Ins/FO = insula/frontal operculum, IFG = inferior frontal gyrus, IPL = inferior parietal lobule, FEF = frontal eye field, SEF = supplemental eye field, MOG = middle occipital gyrus, MT = middle temporal area, IOG= inferior occipital gyrus, SFG = superior frontal gyrus, ITG = inferior temporal gyrus, MFG = middle frontal gyrus.

Region		Brodmann's area	Form						Motion						Working memory					
			size	p(FDR)	z	x	y	z	size	p(FDR)	z	x	y	z	size	p(FDR)	z	x	y	z
Ins/FO	L	13	119	0.008	3.92	−30	18	−2	210	0.03	4.34	−22	26	2	1826	0.013	4.47	−26	30	4
IFG	L		4	0.005	4.79	−38	0	24	76	0.03	3.61	−42	0	28		0.013	4.18	−38	0	26
IPL	R	7, 40	665	0.005	4.35	34	48	32	318	0.03	4.32	38	−42	36	760	0.013	3.98	36	−48	34
																0.028	3.62	26	−68	38
	L		288	0.005	4.77	−18	68	38	692	0.03	4.12	−36	−60	46	1967	0.013	4.63	−22	−68	42
			5							0.03	3.93	−32	−40	36						
FEF	L	6		0.005	4.42	−26	−12	58	95	0.03	3.62	−20	−8	50	344	0.014	3.80	−24	−8	48
	R	6	106	0.007	3.96	48	6	44							1348	0.014	3.70	40	2	50
IFG	R	44, 45, 47	8	0.006	4.13	38	6	24	450	0.03	4.08	46	6	28		0.013	4.25	44	6	26
Insula	R	13	157	0.019	3.29	32	22	2	315	0.03	4.19	28	26	2		0.014	3.70	30	26	4
SEF		32	117	0.005	4.71	8	20	42	104	0.03	3.66	0	18	44	519	0.013	4.11	0	16	46
			9	0.005	4.29	−8	20	30								0.044	2.84	10	28	28
MOG/IOG	L	18, 19, 37	686	0.005	4.81	−44	−70	−10							358	0.013	4.12	−40	−64	−16
MT	L	-							100	0.03	3.77	−36	−64	2						
Declive	L	-													142	0.019	3.43	−30	−70	−30
Culmen	R		46	0.013	3.54	34	−52	−28												
IOG	R	18	47	0.017	3.35	38	−84	−10												
SFG	R	10	49	0.021	3.23	26	44	30							115	0.019	3.45	32	48	30
ITG	R		53	0.024	3.16	28	−68	18												
MFG	L								62	0.03	3.67	−28	48	12						
Thalamus	R														46	0.03	3.12	10	−14	8

NIH-PA Author Manuscript
NIH-PA Author Manuscript
NIH-PA Author Manuscript

Table 2

Loci of differential activation in Form > Motion and Motion > Form contrasts and a trend-level display threshold of $p < 0.001$ (uncorrected) and extent threshold, $k > 20$. . Coordinates in MNI. Size of cluster (number of voxels) and Z scores are also included. Abbreviations: IOG = inferior occipital gyrus, MT = middle temporal area

Region		Brodmann's area	Form > Motion					Motion > Form				
			size	z	z	y	z	size	z	z	y	z
IOG (V4)	R	18, 19	49	3.93	38	−84	−10					
MT (V5)	L	37						171	4.74	−42	−68	4
	R	22, 37						24	3.41	42	−58	4
								50	3.50	54	−42	2
Lingual gyrus (V2)	L	17, 18, 19						42	3.52	−12	−94	−8
Declive	L							83	3.55	−18	−74	−22

NIH-PA Author Manuscript
NIH-PA Author Manuscript
NIH-PA Author Manuscript

Table 3

Loci of activation in Working Memory > Discrimination contrast at a trend-level display threshold of $p < 0.001$ (uncorrected) and an extent threshold, $k > 20$. Coordinates in MNI. Size of cluster (number of voxels) and Z scores are also included. Abbreviations: IPL = inferior parietal lobule, MFG = middle frontal gyrus.

Region		Brodmann's area	Working Memory > Discrimination				
			size	z	x	y	z
IPL	L	7, 40	198	3.91	−28	−62	42
	R		83	3.39	36	−62	40
MFG	L	9, 10, 46	145	3.51	−34	44	14